Swiss J Geosci (2011) 104:455–469
DOI 10.1007/s00015-011-0071-3

Local and regional minimum 1D models for earthquake location and data quality assessment in complex tectonic regions: application to Switzerland

Stephan Husen · Edi Kissling · John F. Clinton

Received: 13 January 2011 / Accepted: 21 June 2011 / Published online: 8 October 2011

Abstract One-dimensional (1D) velocity models are still widely used for computing earthquake locations at seismological centers or in regions where three-dimensional (3D) velocity models are not available due to the lack of data of sufficiently high quality. The concept of the minimum 1D model with appropriate station corrections provides a framework to compute initial hypocenter locations and seismic velocities for local earthquake tomography. Since a minimum 1D model represents a solution to the coupled hypocenter-velocity problem it also represents a suitable velocity model for earthquake location and data quality assessment, such as evaluating the consistency in assigning pre-defined weighting classes and average picking error. Nevertheless, the use of a simple 1D velocity structure in combination with station delays raises the question of how appropriate the minimum 1D model concept is when applied to complex tectonic regions with significant three-dimensional (3D) variations in seismic velocities. In this study we compute one regional minimum 1D model and three local minimum 1D models for selected subregions of the Swiss Alpine region, which exhibits a strongly varying Moho topography. We compare the regional and local minimum 1D models in terms of earthquake locations and data quality assessment to measure their performance. Our results show that the local minimum 1D models provide more realistic hypocenter locations and better data fits than a single model for the Alpine region. We attribute this to the fact that in a local minimum 1D model local and regional effects of the velocity structure can be better separated. Consequently, in tectonically complex regions, minimum 1D models should be computed in sub-regions defined by similar structure, if they are used for earthquake location and data quality assessment.

Keywords Earthquake location · Minimum 1D model · Data quality · Switzerland

Editorial handling: A. Hirt and A.G. Milnes.

S. Husen (✉) · J. F. Clinton
Swiss Seismological Service, ETH Zurich, Sonneggstr. 5,
8092 Zurich, Switzerland
e-mail: husen@sed.ethz.ch

E. Kissling
Institute of Geophysics, ETH Zurich, Sonneggstr. 5,
8092 Zurich, Switzerland

1 Introduction

One-dimensional (1D) velocity models are still widely used for computing earthquake locations, in particular at many seismological centers that monitor seismicity in real-time (e.g. Hutton et al. 2006; Midzi et al. 2010). Since ray-tracing is computationally less demanding in 1D velocity models than in 3D velocity models, the use of 1D velocity models provides very rapid earthquake locations, which becomes important for automatic real-time monitoring of seismicity. Moreover, the lack of data of sufficiently high quality sometimes does not allow the computation of appropriate 3D velocity models for earthquake locations. This becomes important for temporary deployments, where data are only recorded for a limited time (e.g. a few months), but reliable earthquake locations are still needed. For these cases, the computation of a 1D velocity model is the only way to consistently obtain reliable hypocenter locations. Finally, 1D velocity models are the only choice for data quality assessment prior to a 3D tomography study (Husen et al. 2003) and to detect systematic errors in

arrival time data (Maurer et al. 2010). Hence, there is still a need for reliable 1D velocity models in seismology, despite the fact that 3D velocity models are becoming increasingly popular.

The concept of the minimum 1D model has been originally developed to derive reliable initial hypocenter locations and seismic velocities for local earthquake tomography (Kissling 1988; Kissling et al. 1994). The computation of a minimum 1D model explicitly solves the coupled hypocenter-velocity problem, and thus it also provides suitable velocity models for routine earthquake location, where a similar accuracy in earthquake location is required for each single earthquake (Kissling 1988). Moreover, a minimum 1D model can be used for data quality assessment prior to local earthquake tomography (Husen et al. 2003) and to detect systematic errors in arrival time data (Maurer et al. 2010). The latter is due to the fact that a minimum 1D model yields an average minimum data fit and that a 1D model, as opposed to a 3D model, may not absorb systematic errors in arrival time data as it is highly overdetermined.

Minimum 1D models have been successfully computed for several tectonic regions in the world (e.g. Diehl et al. 2009a; Haslinger et al. 1999; Husen et al. 2003; Husen et al. 1999; Husen and Smith 2004; Imposa et al. 2009; Kissling and Lahr 1991). Nevertheless, the use of a simple 1D velocity structure in combination with station delays raises the question how useful the minimum 1D model concept can be when applied to complex tectonic regions with significant three-dimensional (3D) variations in seismic velocities. For example, a relatively high final root mean square (RMS) travel time residual of 0.3 s, compared to an average picking error of 0.2 s, for a minimum 1D model in the Swiss Alpine region was explained with the fact that a significant amount of the 3D velocity structure could not be approximated by a minimum 1D model with station delays (Husen et al. 2003). Similarly, high-quality P-wave arrivals from earthquakes in southern Switzerland and northern Italy recorded at stations in northern Switzerland often show travel-time residuals of several seconds if located with a minimum 1D model (Deichmann, personal communication, 2010).

In order to investigate the applicability of the minimum 1D model concept in tectonically complex regions, we compute minimum 1D models for the Swiss Alpine region. These models are computed for different data sets representing the entire region and three subregions defined by Moho topography. We compare hypocenter locations and travel-time residual distributions for each subregion as computed with the corresponding minimum 1D models with those computed with the minimum 1D model for the entire region. Our results indicate that the subregion-specific "local" minimum 1D models provide hypocenter locations that are more consistent and accurate than those calculated with the "regional" model. Standard deviations of travel-time residual distributions are a factor of two smaller if computed using the subregion-specific minimum 1D models. Consequently, these minimum 1D models are much more appropriate for data quality assessment.

2 Earthquake data and definition of subregions

We use arrival time data of local earthquakes in the Swiss Alpine region for the time period 1984–2008. Data were recorded mainly at stations operated by the Swiss Seismological Service (SED). Data from stations in the neighboring countries were included if available. Prior to 2000 most stations were equipped with single-component (vertical) short-period sensors and analogue data transmission; since 2000 most stations consisted of three-component broadband sensors and digital data transmission. All arrival time data was processed manually at the Swiss Seismological Service. Data for the years 1984–2001 were manually picked by a single experienced seismologist (Husen et al. 2003), whereas data for the years 2002–2008 were picked manually by three experienced seismologists. The quality of each arrival time was estimated by assigning observational weights that correspond to a given uncertainty in picking the arrival time (Table 1). Prior to 2005, arrival times were weighted using a three-class weighting scheme, which changed in 2005 to a four-class weighting scheme. In order to achieve a consistent weighting scheme for the years 1984–2008 arrival time data prior to 2005

Table 1 Observational weights and associated uncertainty interval used by SED and in this study

SED (1984–2004)		SED (since 2005)		This study (merged)	
Weight	Uncertainty interval (s)	Weight	Uncertainty interval (s)	Weight	Uncertainty interval (s)
I (Impulsive)	±0.050	0	±0.025	0	±0.025
E (Emergent)	±0.250	1	±0.050	1 (including I)	±0.050
Q (Questionable)	>0.250	2	±0.100	2	±0.100
		3	±0.200	3 (including E)	±0.200
		4 (rejected)	>0.200	4 (rejected)	>0.200

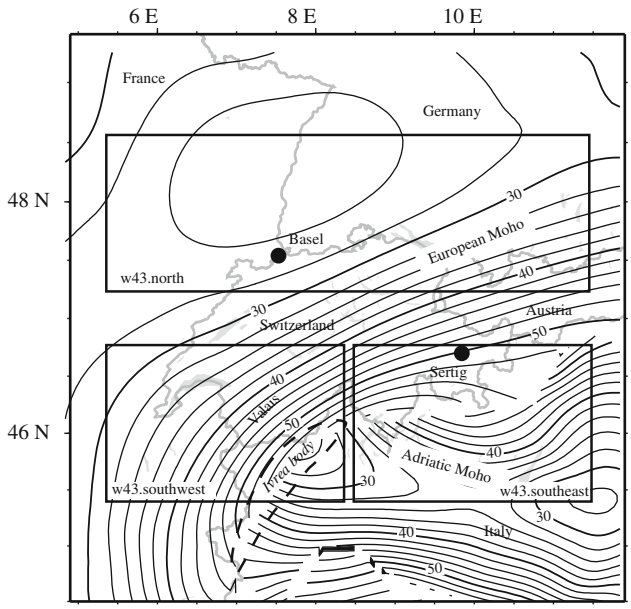

Fig. 1 Map of study area. *Boxes* mark subregions for which local minimum 1D models were computed. *Contour lines* show Moho topography from Waldhauser et al. (1998). Contour interval is 2 km. Discontinuous contour lines are caused by offsets in the Moho. *Dashed line* marks approximate outline of the Ivrea body. Location of geographical places discussed in the text are marked

were re-weighted according to the weighting scheme for the years 2005–2008 (Table 1). Arrival times that were assigned a questionable observational weight (class Q) were not used in this study. We did not include S-wave arrival time data because their number was not sufficient for an inversion for S-wave velocities. This is probably due to the low number of three-component stations prior to 2000 and due to the complexity in picking S-wave arrival times, which often yields a significantly lower number of available phases, compared to available P-wave arrival times for the same data set (Diehl et al. 2009b).

The simultaneous inversion of arrival time data for seismic velocities and hypocenter locations demands the selection of well-locatable hypocenter locations, due to the coupling between seismic velocities and hypocenter locations (Husen et al. 1999; Kissling et al. 1994). We selected a set of 544 earthquakes with a minimum of eight P-wave observations and an azimuthal gap <1,800. This yielded a total of 10,135 P-wave observations with an average reading error of 0.1 s, based on the assigned uncertainty intervals given in Table 1. The set of 544 earthquakes was split into three data sets for the sub-regions of northern, southwestern, and southeastern Switzerland (Fig. 1). The definition of the sub-regions was based on Moho topography: Northern Switzerland is characterized by a shallow Moho between 25 and 35 km depth, whereas southwestern and southeastern Switzerland shows a deep Moho between 40 and 50 km depth. The split between the subregions of southwestern and southeastern Switzerland was necessary because of the presence of the high-velocity Ivrea body in the western Alps and because of the complex Moho topography in the region due to the suture between the European and Adriatic Moho (Fig. 1). The number of earthquakes and observations selected for each subregion is given in Table 2. All three data sets have a similar average reading error of 0.1 s. The distribution of earthquakes and stations for each data set is shown in Fig. 2. It is important to note that all data sets use the same distribution of stations which samples the entire greater Swiss Alpine region. Earthquakes in northern Switzerland occur throughout the entire crust, including the lower crust. Seismicity in southwestern and southeastern Switzerland is mainly restricted to the upper crust (<15 km depth) with a few deep earthquakes in northern Italy (Fig. 2).

3 Minimum 1D models for the Swiss Alpine region

3.1 Concept of the minimum 1D model

The linearized inversion of arrival time data from local earthquakes demands the solution of the coupled hypocenter-velocity problem (Thurber 1992). Linearization requires that starting parameters (seismic velocities and hypocenter locations) are close to the true values. The concept of the minimum 1D model was introduced by Kissling (1988) to compute an initial reference model for a subsequent 3D local earthquake tomography study. A minimum 1D model is computed by simultaneous inversion of arrival time data from local earthquakes for hypocenter locations, seismic velocities, and station delays. Hence, it represents a full solution to the coupled hypocenter-velocity problem. The solution is computed using a

Table 2 Data sets used in this study and final RMS travel time residuals of the corresponding minimum 1D model

Data	Number of earthquakes	Number of observations					Average reading error (s)	Final RMS travel time residuals (s)
		P0	P1	P2	P3	Total		
w43.all	558	2,450	6,523	33	1,129	10,135	0.10	0.30
w43.north	114	1,087	1,474	33	163	2,757	0.10	0.13
w43.southwest	195	563	2,240	0	357	3,160	0.10	0.17
w43.southeast	92	434	780	0	66	1,280	0.09	0.13

P0-P3 refer to observational weights of P-wave arrival time picks as shown in Table 1

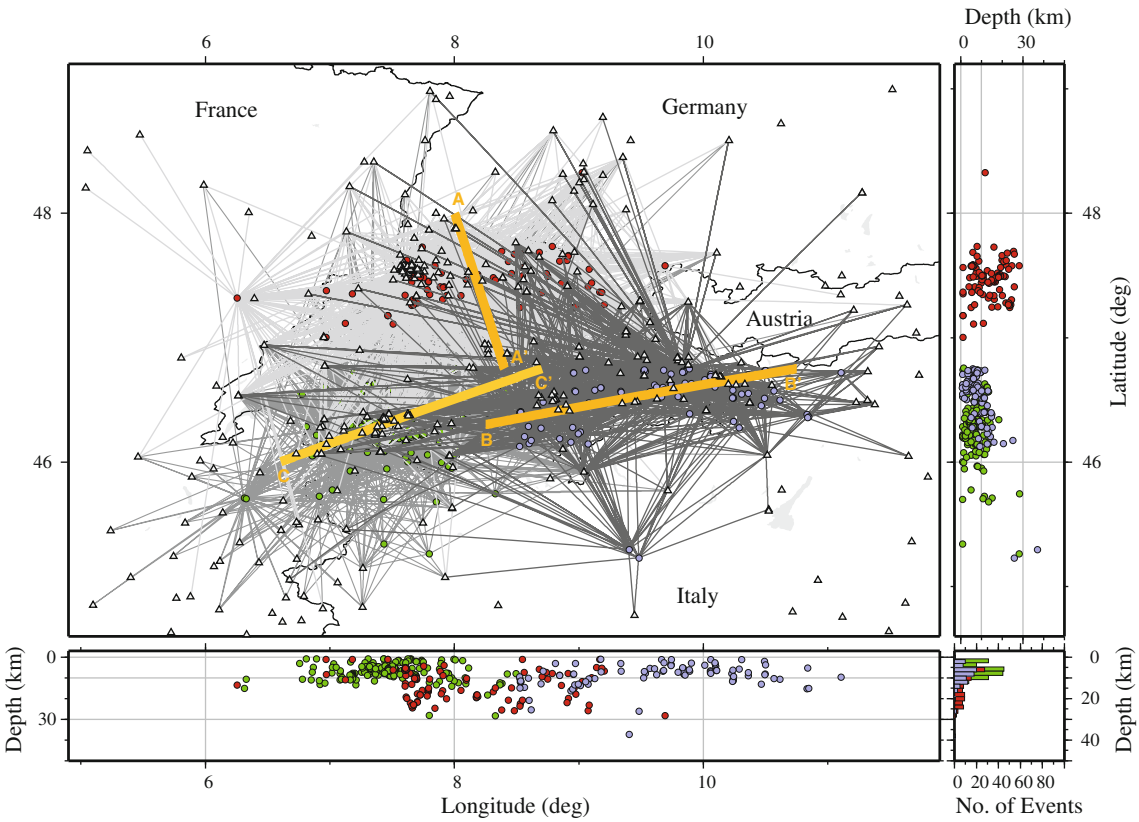

Fig. 2 Hypocenter locations of selected earthquakes for the subregions north (*red circles*), southeast (*light blue circles*), and southwest Switzerland (*green circles*). Stations are marked by *black triangles*. *Gray* and *black lines* show ray paths between epicenters and stations for the different data sets. *Orange lines* mark location of profiles shown in Fig. 7. Only well-locatable hypocenter locations with at least 8 P-wave observations and a GAP $< 180°$ were used. Number of earthquakes and number of observations for each data set are given in Table 2

damped least square approach (Kissling 1988) and each inversion consists of several iterations. The inversion is usually stopped when model adjustments become insignificant and a significant reduction in data variance has been achieved. The latter depends, of course, on the a priori data error. The advantage of using a 1D velocity model, compared to a 3D model, to solve the coupled hypocenter-velocity problem is that non-linearity due to the velocity model is less severe and that, due to the smaller size of the solution space, the full set of linear diagnostics, such as eigenvalues and eigenvectors, can be computed. The term minimum denotes the fact that a minimum 1D model leads to a minimum average RMS travel time residual for all earthquakes in the inversion. This makes the minimum 1D model a very suitable model to detect systematic errors in arrival data caused by phase misidentifications or by wrong station coordinates (Maurer et al. 2010). Since all earthquakes are located with a similar accuracy a minimum 1D model presents also an ideal model for routine earthquake locations, where each earthquake should be located with a similar accuracy. In a minimum 1D model seismic velocities represent averages of the layer velocities as sampled by the distribution of rays within the same depth range (Kissling 1988). Hence, a similar distribution of earthquakes and stations should be used for the minimum 1D model and the 3D tomography. Station delays are included in the inversion to compensate for near-surface velocity heterogeneity and for large-scale velocity variations in the crust. They are computed relative to a reference station (with a delay of zero) and relative to the velocity of the first layer. While station delays are dominated by near-surface geology for stations located within a network, they are dominated by large-scale velocity variations in the crust for stations that are located at the periphery of the network and, hence, show arrival time recordings in a narrow range of azimuths. If the corresponding rays pass through a large velocity anomaly, such as a subducting slab, station delays of these stations will be dominated by the effect of such a velocity anomaly (Husen et al. 1999).

The computation of a minimum 1D model is a trial and error process that involves a wide range of initial models to sample the entire solution space (Kissling et al. 1994). A priori information on main crustal discontinuities needs to be available prior to the inversion to establish an appropriate layering of the minimum 1D model. This can be done by analyzing available controlled source seismology

(CSS) data for main crustal discontinuities, such as the contact between basement and sediments, the Conrad, and the Moho discontinuity. If CSS data is not available arrival time data of selected earthquakes can be plotted and analyzed in a similar fashion as refraction seismology data, e.g. by using phase correlation and cross-over distances to determine the velocity and thickness of main crustal layers (Deichmann 1987). As the process of computing a minimum 1D model can lead to ambiguous results, the final models need to be verified with independent geological information. For example, computed station delays should correlate with local near-surface geology. The stability of a minimum 1D model needs to be tested by a series of tests, including randomly and systematically shifted hypocenter locations as initial hypocenter locations and so-called high-low tests (Husen et al. 1999; Kissling et al. 1994). High-low tests use very low and high velocities as initial models in the inversion. If the minimum 1D model represents a stable minimum in the solution space, final models from these high-low tests will converge to the same minimum 1D model for layers that are well resolved by the data. The quality of a minimum 1D model depends critically on data selection (Kissling 1988). Only well-locatable earthquakes with a large number of observations (>8 P-wave and/or >8 S-wave observations) and a small azimuthal gap between stations (GAP < 180) should be used in the inversion. As the number of unknowns is significantly less than for a 3D inversion, a smaller subset of earthquakes (>100 earthquakes) is usually sufficient to compute a minimum 1D model. This allows only the high-quality data to be selected (e.g. large number of observations per event, observations with smallest reading error) for the computation of a minimum 1D model, thus improving the reliability of the obtained model.

3.2 Computation of the minimum 1D models for Swiss Alpine region

We computed minimum 1D models for each earthquake data set and region as given in Table 2. Each inversion used the same initial velocity model, which is the minimum 1D model computed by Husen et al. (2003) for the same region using an older data set. Compared to the model of Husen et al. (2003), the layering of the minimum 1D models derived in this study was adapted to allow the use of borehole stations from a geothermal experiment in the Basel area (Deichmann and Giardini 2009). This resulted in an increased thickness of first layer to 1 km below sea level and the inclusion of thinner layers (thickness of 5 km instead of 10 km) between 20 and 50 km depth. The latter was necessary for a better parameterization of the velocity gradient across the Moho, which varies between 25 and 50 km depth in the study region. Initial hypocenter locations for each data set were computed using the same minimum 1D model of Husen et al. (2003). Station delays were set to zero at the beginning of each inversion. The computation of each minimum 1D model comprised two inversion runs. In the first run, hypocenter locations were adjusted at every iteration, whereas seismic velocities and station delays were adjusted only every second iteration. Following Kissling et al. (1994), damping was set to 0.01 for hypocenter locations and station delays, and to 0.1 for seismic velocities. The inversion was stopped when model adjustments became insignificant (usually after 6–8 iterations). The goal of the first run was to find the appropriate minimum for each model in terms of seismic velocities, hypocenter locations, and station delays. The second run used seismic velocities and hypocenter locations of the previous run as initial values, and damping was set to 10.0 for seismic velocities (damping for hypocenter locations and station delays were not changed). The use of a higher damping value for seismic velocities prevents large changes to the general velocity structure but it allows for larger changes in hypocenter locations and station delays. For this run, hypocenter locations, seismic velocities, and station delays were adjusted at every iteration. Inversions usually terminated after 2–3 iterations. The goal of the second run was to allow for a finer adjustment of hypocenter locations, seismic velocities, and station delays in the vicinity of the previously found minimum in the solution space. The minimum 1D models for each region after these two runs are shown in Fig. 3 and the final RMS travel time residual is given in Table 2.

The stability of each minimum 1D model was investigated using tests with randomly and systematically shifted hypocenter locations, and with tests that comprised very high and very low seismic velocities as initial models (so called high/low tests, Husen et al. 1999). Results from these tests are not shown for the sake of brevity but discussed in the following. Tests with the randomly and systematically shifted hypocenter locations showed that final hypocenter locations were relocated within 0.5–1 km in epicenter and within 2–3 km in focal depth with respect to the original (unshifted) locations. The high/low tests showed that all models converged to the original seismic velocities within 0.05–0.1 km/s for layers down to 25 km depth. This indicates that seismic velocities for these layers are well constrained as can be expected from the depth distribution of the earthquakes. Most of the earthquakes are located in the depth range 0–15 km depth (Fig. 3). Convergence was poor below 25 km depth for the models w43.southwest and w43.southeast, indicating that seismic velocities at these depths were not well constrained. This can be expected due the low number of earthquakes in this depth range (Fig. 3). The presence of deep earthquakes beneath northern Switzerland yielded a good convergence

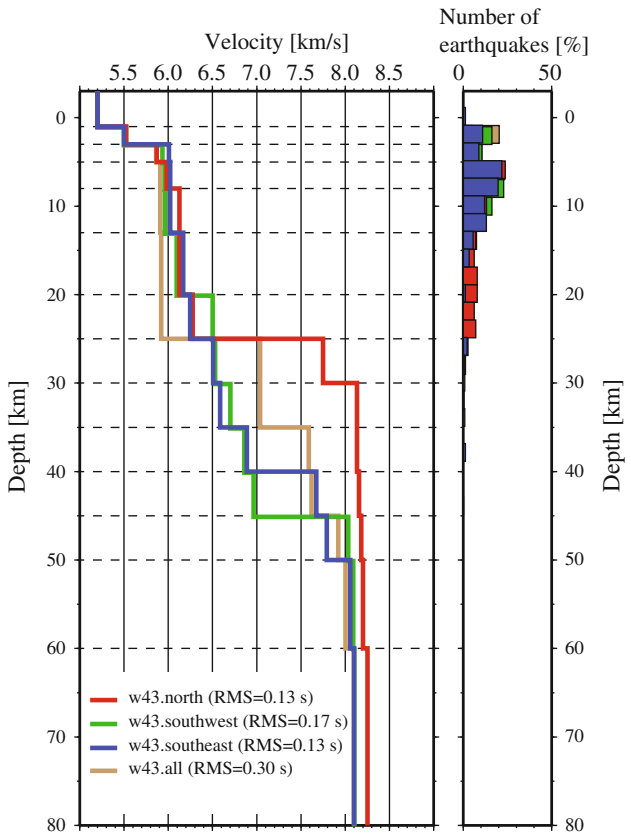

Fig. 3 Final P-wave velocity models after 1-D inversion (*left*) and focal depth distribution (*right*). Models and focal depth distributions for different data sets are shown in different colors as indicated. *Dashed horizontal lines* mark layering in depth. For each model the final RMS travel time residual after 1-D inversion is given

within 0.1–0.2 km/s of the seismic velocities down to 50 km depth for the models w43.north and w43.all. The strong velocity increase between 25.0 and 30.0 km depth in model w43.north is well constrained by the data. This was tested by using input models that had a similar velocity increase at shallower or at greater depth or where the velocity increase was gradual from 20.0 to 30.0 km depth. All these models converged to the velocity model w43.north.

3.3 Velocity structure and data fit of the minimum 1D models

The resulting minimum 1D models do not differ significantly for the upper crust (top 15 km) but show quite different results in terms of the deeper velocity structure (>15 km depth) and final RMS travel time residuals (Fig. 3). The resulting velocity structure of the top 15 km is in good agreement with the minimum 1D model of Husen et al. (2003). This minimum 1D model was computed for the same region using an older data set. Large differences in the velocity structure can be observed for depths greater than 20 km (Fig. 3). The model w43.all, computed for the entire region, shows a gradual increase in seismic velocities from about 5.9 km/s at 25.0 km depth to about 8.0 km/s at 50.0 km depth. No sharp increase in seismic velocities from lower crustal velocities (6.5–6.6 km/s) to upper mantle velocities (8.0–8.1 km/s), which would be indicative for the existence of a clear Moho, is observed for this model. A similar velocity structure for depths greater than 20 km was obtained by Husen et al. (2003). The absence of a clear Moho for the model w43.all can be explained with the Moho topography in the study region. The Moho depth gradually increases from 25.0 km in northern Switzerland to 50.0 km depth in the central Alps (Fig. 1). As a consequence, ray paths in the 20.0–50.0 km depth range are a mixture between those Pg phases sampling the lower crust and Pn phases sampling the upper mantle. For example, ray paths to stations in southern Switzerland originating from earthquakes in northern Switzerland will sample mainly the lower crust due to the deepening of the Moho, while ray paths to stations in northern Switzerland originating from earthquakes in southern Switzerland will sample mainly the upper mantle due to the shallowing of the Moho. Since seismic velocities in a minimum 1D model represent average velocities per layer weighted by the ray distribution at this depth range, the resulting seismic velocities will be higher than lower crustal velocities (>6.5 km/s) but lower than upper mantle velocities (<8.0 km/s). This will lead to a gradual increase in seismic velocities without a clear Moho as observed for model w43.all (Fig. 3).

A clear Moho is present in model w43.north at depths between 25 and 30 km associated with a velocity increase from 6.2 to 8.1 km/s (Fig. 3). This is in good agreement with a priori known Moho depths at 25–30 km beneath northern Switzerland (Fig. 1). The Moho depth in model w43.north is well constrained by the existence of deep earthquakes beneath northern Switzerland (Fig. 3). The models w43.southeast and w43.southwest show evidence for a velocity discontinuity correlated with a Moho at depths of 40 and 45 km, respectively. Although the velocity structure at this depth is not well constrained for these models the observed Moho depths are in good agreement with a priori known Moho depths, which vary between 40 and 50 km depth in southeastern and southwestern Switzerland (Fig. 1). Seismic velocities of the lower crust (30–40 km depth) observed in the model for the entire region are higher than average lower crustal velocities in the models w43.southeast and w43.southwest (6.7–6.9 km/s compared to 6.5 km/s). This is caused by the effects of a significantly dipping Moho beneath Switzerland in combination with observations at stations in northern Switzerland that mainly sample upper mantle velocities at this depth range.

RMS travel time residuals of the minimum 1D models computed for the subregions (w43.north, w43.southeast, w43.southwest) are significantly lower than that for the minimum 1D model computed for the entire region (w43.all, see Table 2). Moreover, the final RMS travel time residual of 0.30 s of the entire region model is three times larger than the average a priori picking error of 0.10 s. The other models achieve RMS travel time residuals that are comparable to the a priori average picking errors (Table 2). A RMS travel time residual that is significantly higher than the a priori reading error can be explained by (a) an inappropriate estimation of the a priori picking error, (b) the fact that the minimum 1D model did not converge, or (c) a significant amount of 3D structure that cannot be approximated by a minimum 1D model with station delays. The first argument can be ruled out as the minimum 1D models for the subregions achieved RMS travel time residuals that are comparable to the a priori picking error. The second argument is also unlikely as the stability of each minimum 1D model was successfully tested. We, therefore, attribute the relatively high final RMS travel time residual to unmodelled 3D structure. Husen et al. (2003) achieved a similar final RMS travel time residual for their model computed for the same region, although the a priori picking error of their data was 0.2 s due to the lower quality of their data. They concluded that the relatively high final RMS travel time residual was due to a significant amount of 3D structure that could not be approximated by a minimum 1D model with station delays. The fact that the minimum 1D models for the subregions achieve final RMS travel time residuals that are comparable to the a priori picking error further supports the idea that unmodelled 3D structure produces a final RMS travel time residual larger than the a priori picking error. Moho topography is less complex in the subregions, which can apparently be well approximated by a minimum 1D model with station delays.

3.4 Station delays of the obtained minimum 1D models

Station delays change remarkably for the different minimum 1D models (Fig. 4). As stated earlier, station delays form an integral part of a minimum 1D model. For a geologically meaningful minimum 1D model they should correlate with local geology for stations with good azimuthal coverage of the observations. They should be

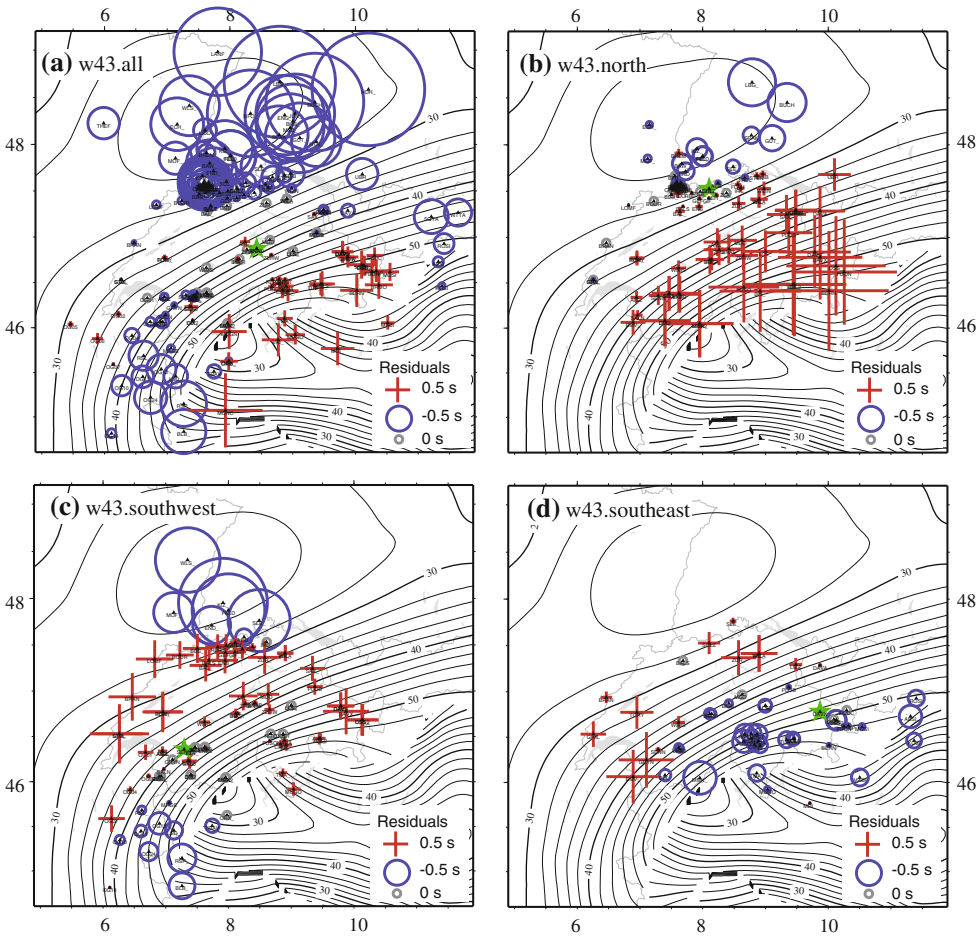

Fig. 4 Final station delays after 1-D inversion for data sets **a** w43.all, **b** w43.north, **c** w43.southwest, and **d** w43.southeast. Station delays are scaled as indicated. Reference station for each data set is marked by a *star*. Moho topography from Waldhauser et al. (1998) is shown by *contour lines*. Station delays are only shown for stations with at least 5 P-wave observations

dominated by large scale deviations in crustal structure from the modelled 1D structure for stations with limited azimuthal coverage of the observations. The magnitude of station delays usually increases with the distance of a station from the center of the network as the difference between modelled and unmodelled structure accumulates with longer ray paths. This effect can be observed for all models (Fig. 4). There are, however, remarkable changes in the pattern of station delays for the different models. For example, station delays in the Valais (western Switzerland) are small for the models w43.all and w43.southwest (Fig. 4a, c) whereas the same stations show predominantly positive delays for the models w43.north and w43.southeast (Fig. 4b, d). These changes can be explained by changes in ray distribution and changes in seismic velocities between the different models as we discuss in the following.

For models w43.all and w43.southwest station delays in the Valais are dominated by the Pg phase of local earthquakes located in the Valais. Hence, these station delays reflect primarily shallow local structure, i.e. outcropping of crystalline basement in the region. In model w43.north, however, station delays are dominated by Pg or Pn phases travelling through the lower crust and upper mantle, respectively. Observations at these stations are modelled as refracted phases in the model w43.north whereas the observed phase is a Pg phase travelling through the mid to lower crust. Consequently, calculated arrival times are smaller than observed travel-times yielding positive station delays (Fig. 4b). On the other hand, station delays for the same stations show a remarkable transition from negative station delays in the eastern Valais to positive station delays in the western Valais in model w43.southeast (Fig. 4d). Observations at the eastern Valias stations are modelled as refracted waves along the Moho at 40 km depth whereas observed travel-times correspond to Pg phases through the mid crust due to the deep Moho in this region. Consequently, calculated travel-times are too large compared to observed travel-times due to a ray path that is longer for the calculated phase. Arrivals at stations in the western Valais are still modelled as refracted waves but due to the large epicentral distance these observations correspond to Pg phases that travel through the lower crust. Hence, differences in ray path are smaller and calculated travel-times are faster compared to observed travel-times yielding positive station delays.

A sharp transition from positive station delays in northern Switzerland to negative station delays in southern Germany for model w43.southwest (Fig. 4c) indicates that observations in southern Germany are dominated by Pn phases, whereas arrivals in northern Switzerland are still mainly Pg phases that travel through the mid to lower crust. These Pg phases are modelled as refracted waves in model w43.southwest yielding travel-times that are smaller compared to the observed travel-times. For the Pn phases, these observations are still modelled as refracted waves but observed arrivals travel through a much thinner lower crust as in the model due to the shallowing of the Moho. This leads to observed travel-times being smaller than calculated arrival times and, hence, to the observed negative station delays. The sharp transition between positive station delays in northern Switzerland and negative station delays in southern Germany is not visible in model w43.all, since, for this model, arrivals at these stations are a mixture of Pg phases from local earthquakes in northern Switzerland and Pn phases from distant earthquakes in southwestern Switzerland. Model w43.southwest does not include observations from local earthquakes in northern Switzerland.

In summary, the observed patterns in station delays agree well with near-surface geology for stations with good azimuthal coverage of the observations and with the observed Moho topography for stations with limited azimuthal coverage of the observations. Since differences between the minimum 1D models are largest for the deeper velocity structure (>25 km depth) the largest differences in station delays between the model are observed for stations located at the edge of the network. These differences are caused by the existing Moho topography in combination with the 1D velocity structure of each model.

4 Discussion

In the following we will discuss the performance of each minimum 1D model for earthquake location and for data quality assessment.

4.1 Earthquake locations

In order to study the performance of the different minimum 1D model with respect to earthquake locations we relocated each earthquake data set with the corresponding minimum 1D model including station delays. As we are mainly interested in the performance of the regional 1D model with respect to the local minimum 1D models for the different subregions we computed differences in latitude, longitude, and focal depth between hypocenter locations obtained with the regional and the corresponding local minimum 1D models. Formal location errors were computed from the half-axes of the 68% confidence error ellipsoid as computed by the NonLinLoc software (Lomax et al. 2000). These comparisons will not allow an assessment of the location accuracy of each model, as this can only be done by relocating events, for which ground truth information is available, e.g. explosions or mine blasts

(Bondar et al. 2004; Husen et al. 1999). Nevertheless, by comparing hypocenter locations of earthquakes for which hypocenter locations have been validated using independent information, location accuracy of the local and regional minimum 1D models can be compared.

As expected, average RMS travel time residuals and individual earthquake RMS travel time residuals are reduced by a factor of two when earthquakes are relocated using the local minimum 1D model (Fig. 5). This is due to the fact that the local minimum 1D models yield a better data fit, as discussed in the previous section. Hypocenter locations, however, do not show large systematic shifts when they are relocated using the local minimum 1D models. Mean shifts in epicenter location and focal depth are of the order of 2 km and in the range of 1–4 km, respectively. These shifts are smaller or in the range of the corresponding error as given by the 68% confidence error ellipsoid. Shifts in epicenter location are comparable for all three data sets (Fig. 6) indicating that the influence of the velocity model on epicenter location is small for well constrained hypocenter locations with a GAP $< 1{,}800$ and at least eight P-wave observations. With respect to focal depth, the data sets show quite different results (Fig. 6). Average shift in focal depth is smallest for data set w43.southwest (0.7 km) and largest for data set w43.north (3.5 km). On the other hand, average error in focal depth is largest for data sets w43.southwest (5.1 km) and w43.southeast (6.5 km), whereas it is smallest for data set w43.north (3.2 km). This is probably due to a larger number of deeper events in data set w43.north, which show a more favourable ratio of focal depth to distance to the closest station. Focal depth is typically well constrained if at least one observation is within a focal depth's distance (Chatelain et al. 1980; Husen et al. 2003). Therefore, average shifts in focal depths are insignificant for data sets

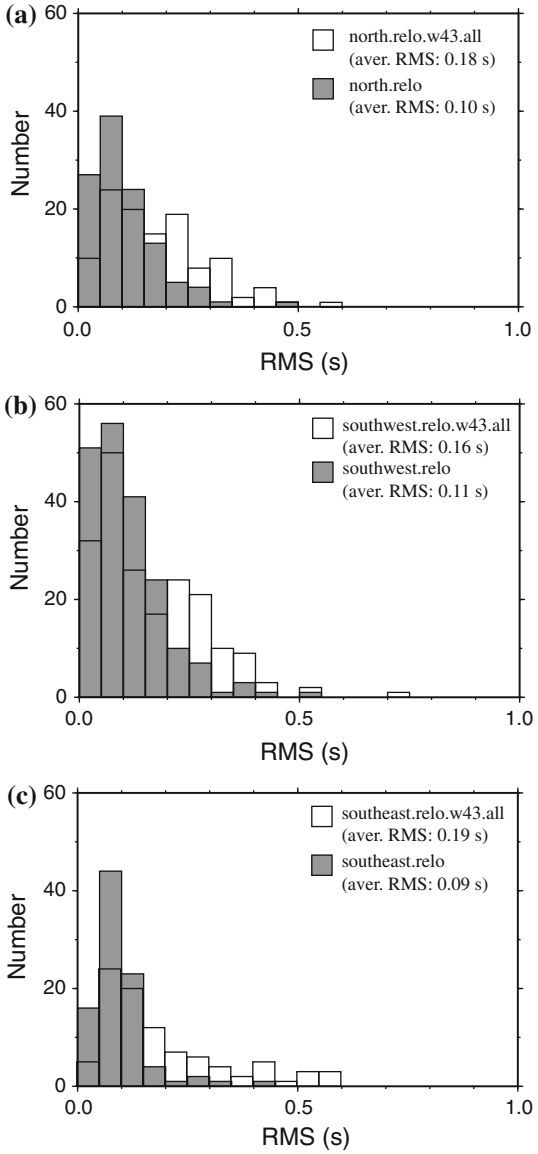

Fig. 5 Histograms of hypocenter RMS travel time residuals for data sets **a** w43.north, **b** w43.southwest, and **c** w43.southeast. RMS travel time residual is computed for each hypocenter location after relocation with the corresponding local minimum 1D model (*gray bars*) and with regional minimum 1D model (*open bars*). Average RMS travel time residual is given for each data set

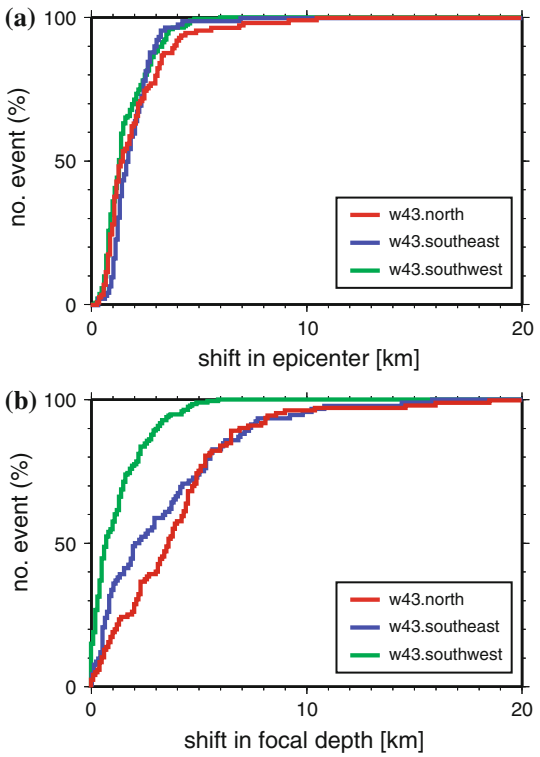

Fig. 6 Cumulative plot of shifts in **a** epicenter and **b** focal depth for different data sets. Shifts are computed between hypocenter locations computed with the corresponding local minimum 1D model and with regional minimum 1D model. Different data sets are shown by different colors as indicated

w43.southeast and w43.southwest; but focal depths are shifted significantly and systematically to more shallow depth for data set w43.north. This observation is also constrained by investigating cumulative plots of shifts in epicenter and focal depth (Fig. 6). About 62 and 44% of the earthquakes in data set w43.north are shifted less than their corresponding average error in epicenter and in focal depth, respectively. For data sets w43.southeast and w43.southwest these numbers are 70 and 86%, and 73 and 99%, respectively.

The observation that shifts in focal depth are largest for earthquakes in northern Switzerland can be explained by the fact that changes in the velocity model are also largest for model w43.north (Fig. 3). Model w43.north shows a clear Moho at 25–30 km depth, whereas model w43.all shows a gradual increase in seismic velocities from 25 to 50 km depth. This change in the velocity model strongly affects deep earthquakes in northern Switzerland, that are located close to the Moho. Focal depths for these earthquakes are often below the Moho when relocated using model w43.all; they are all located above the Moho when relocated using model w43.north (Fig. 7a). The observation of clear PmP phases for these earthquakes confirms that they are in fact located above the Moho and not below the Moho (Deichmann 1987). Changes in station delays between models w43.all and w43.north can also strongly affect focal depth of earthquakes located in the crust. For example, a series of earthquakes induced by a geothermal project in Basel were shifted on average by 7 km to shallower depth when using the model w43.north and station delays (Fig. 7a). Focal depths obtained using model w43.north are in the depth range 5.0–5.5 km, which is consistent with the injection of water for reservoir stimulation between 4.5 and 5 km depth (Deichmann and Giardini 2009). Nearby stations in the Basel region showed large negative station residuals (about −1.0 s) for model

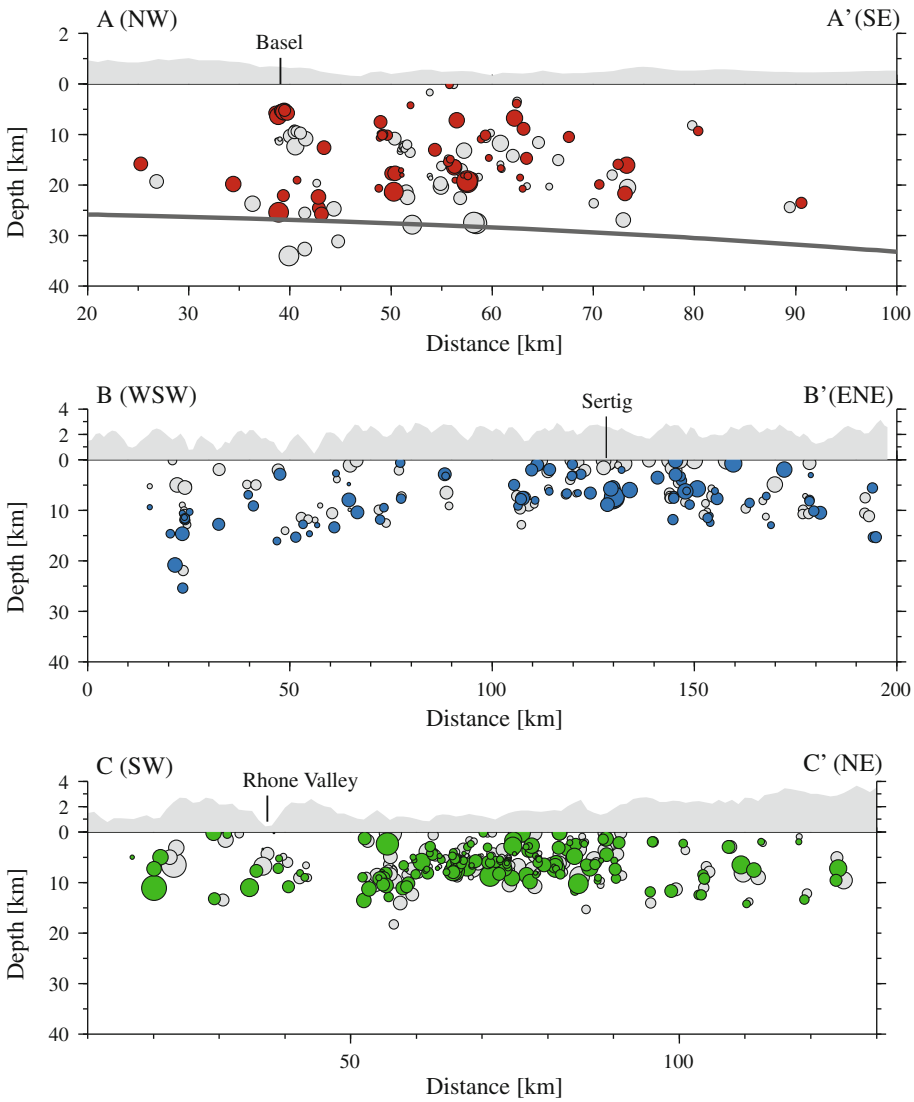

Fig. 7 Vertical cross sections of hypocenter locations in north (*top*), southeast (*middle*), and southwest (*bottom*) Switzerland. See Fig. 2 for location of profiles. Earthquakes within 50 km of each profile have been projected. *Colored circles* denote hypocenter locations computed with the corresponding local minimum 1D models; *gray circles* denote hypocenter locations computed with the regional minimum 1D model. Topography along cross section is shown on *top* for reference. Locations discussed in the text are marked. *Dipping black line* in top vertical cross section outlines Moho depth along the profile; Moho depths are taken from Waldhauser et al. (1998)

w43.all, whereas station delays were small for model w43.north (Fig. 4). These large changes in station delays in combination with changes in the velocity models (Fig. 3) caused a strong shift to a shallower focal depth.

Shift in focal depths for earthquakes in southeastern Switzerland are mainly caused by changes in station delays, since the velocity models w43.all and w43.southeast only differ moderately. Stations in the northern Alpine foreland show large positive station delays (in the range 0.5–0.7 s) in the model w43.southeast, whereas the same stations show small station delays in the model w43.all (Fig. 4). Station delays of model w43.southeast for these stations are dominated by Pg phases from earthquakes in southeastern Switzerland that travel through the lower crust. These station delays compensate for seismic velocities in the lower crust that are probably lower than 6.5–7.0 km/s as given in model w43.southeast. Station delays of model w43.all for stations in the northern Alpine foreland are a mixture between lower crustal Pg phases from distant earthquakes in southeastern and southwestern Switzerland, and upper crustal Pg phases from local earthquakes in northern Switzerland. Since station delays are small, observations at stations in the northern Alpine foreland from earthquakes in southeastern Switzerland often show large positive travel-time residuals when relocated with model w43.all. Due to their downward orientated take-off angles, these observations place important constrains on focal depth. In combination with the observed large positive travel-time residuals, focal depth estimates for these earthquake can be unreliable. As an example, the Ml = 3.9 2003 earthquake of Sertig, close to the village Sertig Doerfli, 10 km south of Davos (GR), is located at a depth of 7.6 km using the model w43.southeast; the same earthquake is located at a depth of 0.2 km using the model w43.all (Fig. 7b). Based on P- and S-wave arrivals at a nearby station (2 km epicentral distance) focal depth for this event was estimated at 6–8 km (Deichmann et al. 2004), which is consistent with the focal depth computed using model w43.southeast.

Shifts in focal depths of earthquakes in southwestern Switzerland are smallest from all subregions (Fig. 7c). These small shifts are in agreement with the observed moderate differences between the velocity structure of models w43.southwest and w43.all (Fig. 3). Moreover, and in contrast to model w43.southeast, station delays show similar patterns in model w43.southwest and w43.all. The similarities in velocity structure and station delays between model w43.southwest and w43.all are probably caused by the large number of earthquakes in data set w43.southwest compared to the other data sets. As a consequence, the velocity structure and station delays of model w43.all are dominated by the large number of earthquakes in subregion w43.southwest.

4.2 Data quality assessment

A key element in assessing data quality of local earthquake data (e.g. consistency in assigning observational errors, average picking error) is the distribution of travel-time residuals computed using a minimum 1D model and station delays. For consistently picked data, travel-time residuals should follow a Gaussian distribution and the corresponding mean and standard deviation should increase gradually with increasing observational error (Husen et al. 2003). Travel-time residuals that are significantly larger than the associated uncertainty interval are indicative of blunders and should be checked. It is important to note, that the use of travel-time residuals for data quality assessment is only valid if they are computed using a minimum 1D model. The reason is that a minimum 1D model represents a solution to the coupled hypocenter-velocity problem in which all earthquakes are located with equal precision (Kissling 1988). Other 1D velocity models derived from a priori information, such as controlled source seismology data, usually do not represent a solution to the coupled hypocenter-velocity problem.

Figure 8 shows the distribution of travel-time residuals of the data set w43.north for different observational weights. Travel-time residuals were computed using the local minimum 1D model w43.north and the regional minimum 1D model w43.all, including station delays. Residual distributions look similar for the other data sets but they are not shown for the sake of brevity. Primary statistical parameters of the residual distributions for all models are listed in Table 3. The relatively small numbers of observations with weight 0 compared to weight 1, and with weight 2 compared to weight 3, is due to the fact that the weights 0 and 2 have only been assigned since 2005. Prior to 2005 data were picked using only weights 1 and 3 (Table 1). Travel-time residuals computed with the local minimum 1D models show a significantly narrower distribution for observational weights 0 and 1, as indicated by a factor of two smaller standard deviation. Travel-time residual distributions for observational weight 3 are similar for both models. This indicates that observations with a weight of 3 are problematic and may contain a large number of inconsistently picked arrival times. Although standard deviations gradually increase with increasing observational weight for both models, they are too large compared to the corresponding uncertainty intervals for the regional model w43.all (Table 3). This is caused by a large number of observations that show travel-time residuals significantly larger than the associated uncertainty intervals. As an example, the Ml = 3.9 2003 earthquake of Sertig, GR, shows consistently large positive travel-time residuals for stations in southern Germany (Fig. 9) when located using the regional minimum 1D model w43.all. This could be interpreted as being caused by phase misidentification, e.g.

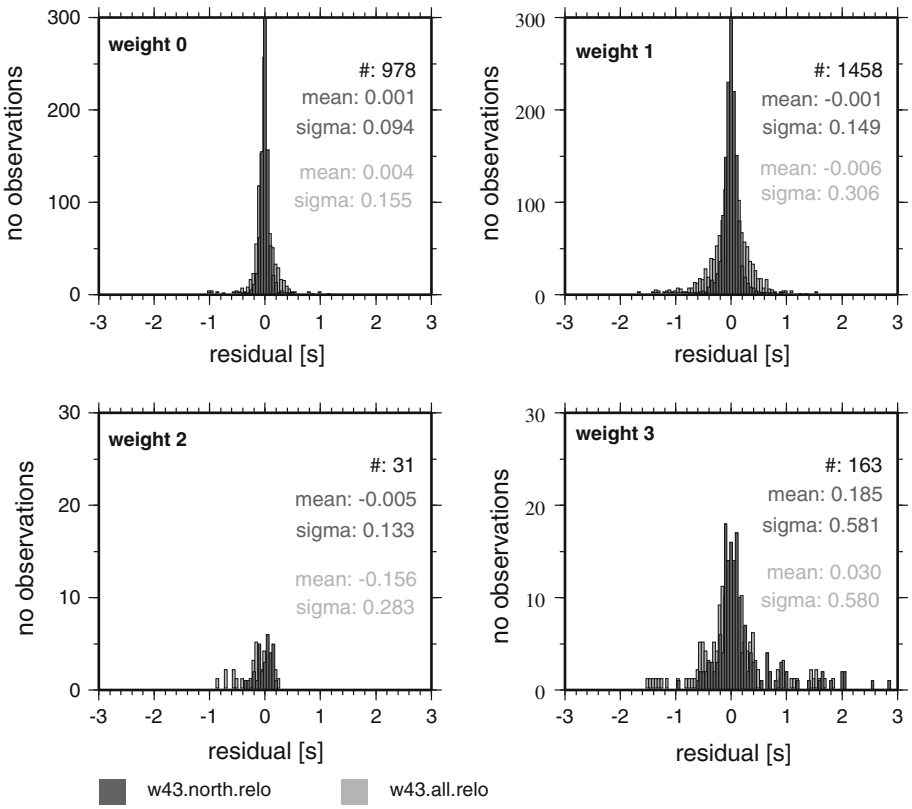

Fig. 8 Histograms of travel-time residuals for different observational weights as indicated. Travel-time residuals were computed using the local minimum 1D models w43.north (*dark gray*) and the regional minimum 1D model w43.all (*light gray*). For each histogram the number of observations, mean and standard deviation (sigma) are given. See Table 3 for primary statistical parameters of all data sets

Table 3 Primary statistical parameters of travel-time residuals for three different data sets

	Observational weight											
	w43.north				w43.southeast				w43.southwest			
	0	1	2	3	0	1	2	3	0	1	2	3
Number	978	1,458	31	163	434	780	0	66	563	2,240	0	357
Mean (s)	0.00	0.00	0.01	0.19	0.00	0.00	–	0.01	0.00	0.00	–	0.11
	0.00	−0.01	−0.16	0.03	0.00	0.13	–	0.16	0.00	0.01	–	0.21
SD (s)	0.094	0.15	0.13	0.58	0.08	0.19	–	0.22	0.09	0.19	–	0.43
	0.16	0.31	0.28	0.58	0.15	0.43	–	0.61	0.14	0.28	–	0.55
Min. (s)	−0.8	−0.7	−0.3	−1.0	−0.4	−1.1	–	−0.9	−0.6	−1.5	–	−1.0
	−1.0	−1.6	−0.8	−1.5	−0.5	−1.3	–	−0.9	−0.7	−1.4	–	−1.2
Max. (s)	1.1	1.3	0.2	2.8	0.5	1.2	–	0.6	0.4	1.7	–	2.5
	1.0	1.6	0.3	1.8	0.8	2.3	–	2.3	1.0	1.7	–	3.2

Earthquakes were relocated using the corresponding local minimum 1D model (top row) and using the regional minimum 1D model (bottom row)

the small-amplitude Pn phase was missed and the large-amplitude PmP phase was picked instead. A reduced record section of the earthquake, however, reveals that observations at stations in southern Germany were correctly identified and picked as Pn arrivals (Fig. 10). The corresponding travel-time residuals computed with the local minimum 1D model w43.southeast are small indicating that arrival times were picked correctly (Fig. 9). This example demonstrates that observations could be falsely identified as blunders if the regional minimum 1D model w43.all was used for data quality assessment.

5 Conclusions

We computed one regional and three local minimum 1D models for Switzerland and its surrounding region. The local minimum 1D models yield a RMS travel time

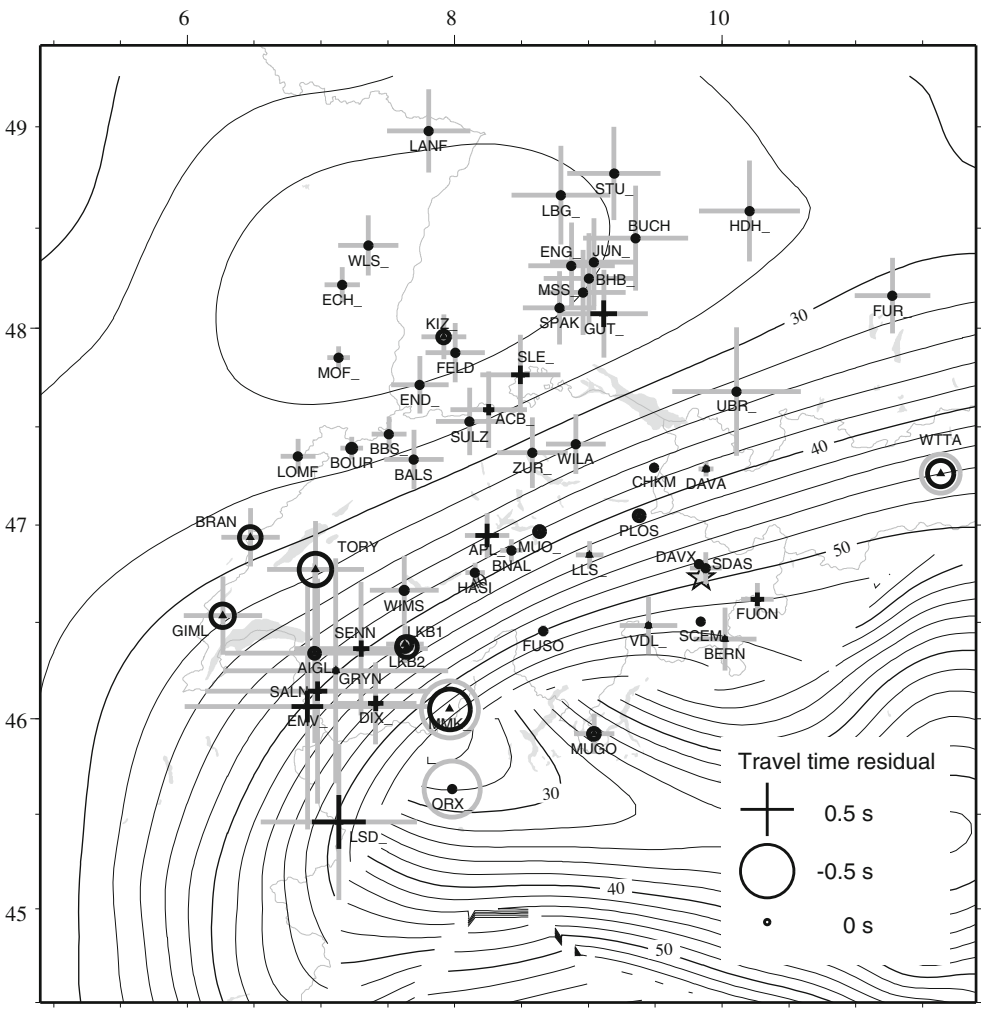

Fig. 9 Travel-time residuals for the 2003 Ml = 3.9 Sertig, GR, earthquake (*star*). Travel-time residuals were computed using the local minimum 1D models w43.southeast (*black*) and the regional minimum 1D model w43.all (*gray*). Travel-time residuals are scaled as indicated. Moho topography from Waldhauser et al. (1998) is shown by *contour lines*. Note the high number of large travel-time residuals for the regional minimum 1D model

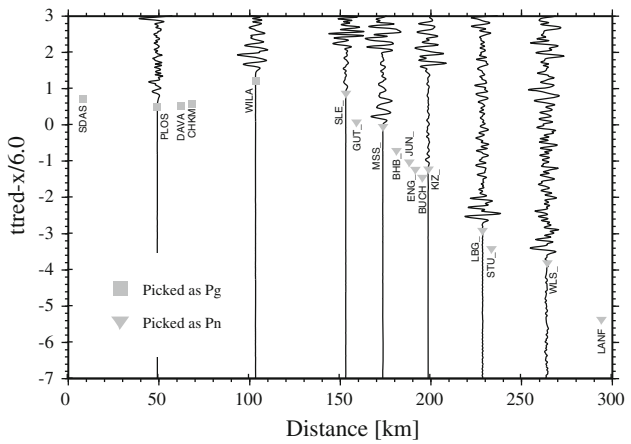

Fig. 10 Velocity reduced record section of the 2003 Ml = 3.9 Sertig, GR, earthquake. Different symbols denote different phases as picked by the analyst. For a few example stations waveforms of the vertical component are shown. Waveforms are band-pass filtered (1–10 Hz) and amplitudes are normalized to maximum amplitude of each trace. See Fig. 9 for location of stations. Arrivals starting at station SLE are correctly identified and picked as Pn arrivals

residual that is smaller by a factor of two compared to the regional minimum 1D model. In contrast to the regional minimum 1D model, the velocity structure of the local minimum 1D models shows a clear Moho that is consistent with previous results (Husen et al. 2003; Waldhauser et al. 1998). Station delays computed with the local minimum 1D models are also locally more consistent with the crustal structure. A clear transition from positive station delays for stations located in northern Switzerland to negative station delays for stations in located in southern Germany as observed for the local minimum 1D models w43.north and w43.southwest is in agreement with the transition from first arriving Pg phases at station located in northern Germany to first arriving Pn phases at stations located in southern Germany. Such a clear transition is not visible for the regional model w43.all as station delays at these stations consist of a mixture between upper crustal Pg phases from local earthquakes in northern Switzerland and lower crustal Pg and Pn phases from distant earthquakes in southern Switzerland.

Changes in the velocity structure and in the station delays between the regional and the local minimum 1D

models yield shifts in hypocenter locations. On average, these shifts are smaller than the associated formal location error as given by the 68% confidence ellipsoid, except for earthquakes in northern Switzerland. Deep earthquakes in northern Switzerland are moved consistently to above the Moho if relocated with the corresponding local minimum 1D model, which is in agreement with the observed PmP phases and a relatively short cross-over distance between the Pg and the Pn phase. Individual hypocenter locations, in particular those that show observations at large distances, are also more consistent with independent information if they are relocated with the corresponding local minimum 1D model.

Distributions of travel-time residuals show similar statistics for the regional and local minimum 1D models, e.g. similar extreme values and increasing standard deviations with increasing observational weight. Compared to the assigned uncertainty interval, however, standard deviations of the travel-time residual distributions computed with the regional minimum 1D model for observational weights 0 and 1 are large. This leads to a larger number of observations that, judged on their travel-time residuals, would be falsely interpreted as blunders if the regional minimum 1D model is be used for data quality assessment.

Our results show that for complex tectonic regions, such as the Swiss Alpine region with strongly varying Moho depths, minimum 1D models computed for selected subregions outperform a regional minimum 1D model. Earthquake locations derived with the local minimum 1D models are more consistent and realistic, and the data fit significantly better, leading to a more reliable assessment of data quality. The improved performance of the local minimum 1D models can be attributed to a better representation of the local velocity structure.

Acknowledgments Data from foreign stations used in this study were kindly provided by the following institutions: BED (Ludwig-Maximilians-University, Munich), GERESS (Hannover), GRSN/SZGRF (Erlangen), INGV/MEDNET (Rome), Landes-Erdbebendienst (Freiburg i. B.), OGS/CRS (Udine/Trieste), RENASS (Strasbourg), RSNI/DipTeris (Genova), SED (Zurich), SISMALP (Grenoble), TGRS (Nice) and ZAMG (Vienna). Access to the data of the borehole sensors in Basel was granted by Geopower Basel AG. We thank Nicolas Deichmann for his efforts in picking arrival times and for discussions. Most of the figures were made using the Generic Mapping Tool by Wessel and Smith (1995). We thank David Booth, A.G. Milnes, and one anonymous reviewer for their constructive and helpful reviews.

References

Bondar, I., Myers, S. C., Engdahl, E. R., & Bergman, E. A. (2004). Epicentre accuracy based on seismic network criteria. *Geophysical Journal International, 156*, 483–496.

Chatelain, J. L., Roecker, S. W., Hatzfeld, D., & Molnar, P. (1980). Micro-earthquake seismicity and fault plane solutions in the Hindu Kush region and their tectonic implications. *Journal of Geophysical Research, 85*, 1365–1387.

Deichmann, N. (1987). Focal depths of earthquakes in northern Switzerland. *Annales Geophysicae Series B-Terrestrial and Planetary Physics, 5*, 395–402.

Deichmann, N., Baer, M., Braunmiller, J., Cornou, C., Fäh, D., Giardini, D., et al. (2004). Earthquakes in Switzerland and surrounding regions during 2003. *Eclogae Geologicae Helvetiae, 97*, 447–458.

Deichmann, N., & Giardini, D. (2009). Earthquakes Induced by the stimulation of an enhanced geothermal system below Basel (Switzerland). *Seismological Research Letters, 80*, 784–798.

Diehl, T., Deichmann, N., Kissling, E., & Husen, S. (2009a). Automatic S-wave picker for local earthquake tomography. *Bulletin of the Seismological Society of America, 99*, 1906–1920.

Diehl, T., Kissling, E., Husen, S., & Aldersons, F. (2009b). Consistent phase picking for regional tomography models: application to the greater Alpine region. *Geophysical Journal International, 176*, 542–554.

Haslinger, F., Kissling, E., Ansorge, J., Hatzfeld, D., Papadimitriou, E., Karakostas, V., et al. (1999). 3D crustal structure from local earthquake tomography around the Gulf of Arta (Ionian region, NW Greece). *Tectonophysics, 304*, 201–218.

Husen, S., Kissling, E., Deichmann, N., Wiemer, S., Giardini, D. & Baer, M. (2003). Probabilistic earthquake location in complex three-dimensional velocity models: application to Switzerland. *Journal of Geophysical Research*. doi:10.1029/2002JB001778.

Husen, S., Kissling, E., Flueh, E., & Asch, G. (1999). Accurate hypocentre determination in the seismogenic zone of the subducting Nazca Plate in northern Chile using a combined on-/offshore network. *Geophysical Journal International, 138*, 687–701.

Husen, S., & Smith, R. B. (2004). Probabilistic earthquake relocation in three-dimensional velocity models for the Yellowstone National Park Region, Wyoming. *Bulletin of the Seismological Society of America, 94*, 880–896.

Hutton, K., Hauksson, E., Clinton, J., Franck, J., Guarino, A., Scheckel, N., et al. (2006). Southern California seismic network update. *Seismological Research Letters, 77*, 389–395.

Imposa, S., Fourno, J.-P., Raffaele, R., Scaltrito, A., & Scarfi, L. (2009). Accurate hypocentre locations in the Middle-Durance Fault Zone, South-Eastern France. *Central European Journal of Geosciences, 1*, 416–423.

Kissling, E. (1988). Geotomography with local earthquake data. *Reviews of Geophysics, 26*, 659–698.

Kissling, E., Ellsworth, W. L., Eberhart-Phillips, D., & Kradolfer, U. (1994). Initial reference models in local earthquake tomography. *Journal of Geophysical Research, 99*, 19635–19646.

Kissling, E., & Lahr, J. C. (1991). Tomographic image of the Pacific slab under southern Alaska. *Eclogae Geologicae Helvetiae, 84*, 297–315.

Lomax, A., Virieux, J., Volant, P., & Berge-Thierry, C. (2000). Probabilistic Earthquake Location in 3D and Layered Models. In C. H. Thurber & N. Rabinowitz (Eds.), *Advances in Seismic Event Location* (pp. 101–134). Dordrecht: Kluwer Academic Publishers.

Maurer, V., Kissling, E., Husen, S., & Quintero, R. (2010). Detection of systematic errors in travel-time data using a minimum 1D model: application to Costa Rica seismic tomography. *Bulletin of the Seismological Society of America, 100*, 629–639.

Midzi, V., Saunders, I., Brandt, M. B. C., & Molea, T. (2010). 1-D velocity model for use by the SANSN in earthquake location. *Seismological Research Letters, 81*, 460–466.

Thurber, C. H. (1992). Hypocenter velocity structure coupling in local earthquake tomography. *Physics of the Earth and Planetary Interiors, 75*, 55–62.

Waldhauser, F., Kissling, E., Ansorge, J., & Mueller, S. (1998). Three-dimensional interface modelling with two-dimensional seismic data: the Alpine crust-mantle boundary. *Geophysical Journal International, 135*, 264–278.

Wessel, P., & Smith, W. H. F. (1995). New version of the generic mapping tool released. *EOS Transactions American Geophysical Union, 76*, 329.